MATERIALS SCIENCE

Electronic quality factor for thermoelectrics

Xinyue Zhang[1]*, Zhonglin Bu[1]*, Xuemin Shi[1]*, Zhiwei Chen[1], Siqi Lin[1], Bing Shan[1], Maxwell Wood[2], Alemayouh H. Snyder[2], Lidong Chen[3], G. Jeffrey Snyder[2†], Yanzhong Pei[1†]

Development of thermoelectrics usually involves trial-and-error investigations, including time-consuming synthesis and measurements. Here, we identify the electronic quality factor B_E for determining the maximum thermoelectric power factor, which can be conveniently estimated by a single measurement of Seebeck coefficient and electrical conductivity of only one sample, not necessarily optimized, at an arbitrary temperature. We demonstrate that thousands of experimental measurements in dozens of materials can all be described by a universal curve and a single material parameter B_E for each class of materials. Furthermore, any deviation in B_E with temperature or doping indicated new effects such as band convergence or additional scattering. This makes B_E a powerful tool for evaluating and guiding the development of thermoelectrics. We demonstrate the power of B_E to show both p-type GeTe alloys and n-type Mg_3SbBi alloys as highly competitive materials, at near room temperature, to state-of-the-art Bi_2Te_3 alloys used in nearly all commercial applications.

INTRODUCTION

Without any emissions or moving parts, thermoelectricity, which enables a direct conversion between heat and electricity, is considered as a clean and sustainable technology for both power generation and refrigeration (*1*). Sufficient conversion efficiency requires materials of high thermoelectric figure of merit, $zT = S^2\sigma T/(\kappa_E + \kappa_L)$, where S, T, σ, κ_E, and κ_L are the Seebeck coefficient, the absolute temperature, the electrical conductivity, and the electronic and lattice component of the thermal conductivity, respectively. The thermoelectric power factor ($S^2\sigma$) is frequently used to describe the primary electronic terms determining zT.

$S^2\sigma$ depends on the band structure, charge scattering, and the doping level of a material, leading its quantity to be a collection of many parameters (*2*) including band degeneracy (*3*), effective mass (*4*), scattering factor (*2*), Fermi level (*2*), and elastic constants (*5*). None of these parameters can be easily determined or used as a complete descriptor for $S^2\sigma$. In addition, because $S^2\sigma$ does not include κ_E, it does not describe all the effects transporting electrons have on zT and does not optimize at the same doping as zT (*6*). This leads the traditional development of thermoelectric materials to involve repeated experiments including synthesis, characterization, and property measurements, which includes some modeling/calculations because of the reoptimization of the materials required for each target temperature. The procedure and models will often differ because of the breadth, complexity, and diversity of the crystal structures, microstructures, and compositions of materials (*7*).

To advance thermoelectrics more efficiently, here, we collect thousands of Seebeck coefficient and conductivity datasets from dozens of thermoelectric materials, at various temperature and degenerate doping, but not necessarily optimized. Such a "big-data" investigation unexpectedly shows that all scaled power factor $S^2\sigma/\overline{B_E}$ follow a universal curve with varying S (Fig. 1). Here, $\overline{B_E}$ is a temperature and doping-independent average electronic quality factor for all samples of the same class (the same parent compound with a rigid band structure). Thus, the difference in power factor, $S^2\sigma$, for different materials can be interpreted simply as due to a difference in B_E or Fermi level as measured by S.

This electronic quality factor B_E can be conveniently estimated from a single set of Seebeck coefficient and conductivity data at any temperatures for a sample that was not necessarily optimized. Because B_E is temperature independent for ideal thermoelectric materials, a single parabolic band (including well-aligned multiple bands) transport with acoustic phonon scattering (SPB-APS) in extrinsic conduction region, any variation in B_E with temperature

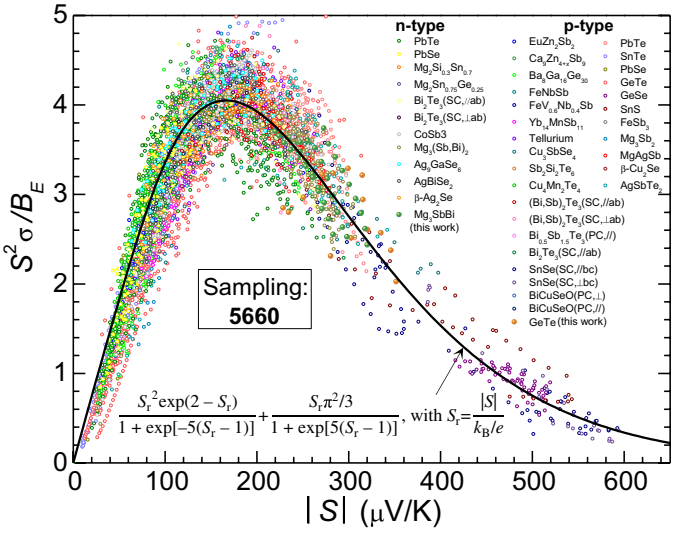

Fig. 1. Scaled power factor versus Seebeck coefficient for thermoelectrics. The experimental thermoelectric power factor $S^2\sigma$ divided by the average electronic quality factor $\overline{B_E}$ follows a universal curve for dozens of thermoelectrics with various types of dopants and additives. This represents thousands of measured results at various temperatures and doping concentrations. Data for anisotropic materials are collected as well. SC, single crystals; PC, polycrystals. Detailed references are given in fig. S4.

[1]Key Laboratory of Advanced Civil Engineering Materials of Ministry of Education, School of Materials Science and Engineering, Tongji University, 4800 Caoan Rd., Shanghai 201804, China. [2]Department of Materials Science and Engineering, Northwestern University, Evanston, IL 60208, USA. [3]State Key Laboratory of High Performance Ceramics and Superfine Microstructure, Shanghai Institute of Ceramics, CAS, Shanghai 200050, China.
*These authors contributed equally to this work.
†Corresponding author. Email: jeff.snyder@northwestern.edu (G.J.S.); yanzhong@tongji.edu.cn (Y.P.)

indicates the presence of unusual effects such as band convergence, additional charge scattering, and bipolar conduction (Fig. 2). This enables B_E as an extremely easily accessible electronic parameter for guiding the advancement of thermoelectrics, with notably reduced loads on experiments.

Furthermore, the electronic quality factor B_E fully describes the electronic contribution to the thermoelectric quality factor $B = B_E T/\kappa_L$ that determines zT and its maximum (zT_{max}) for a material (sections S1 and S2). With the knowledge of T-dependent lattice thermal conductivity (κ_L), B_E offers a full prediction of zT at any temperature and doping level. An analysis of $B_E T/\kappa_L$ at room temperature reveals that both n-type Mg_3Sb_2 alloys (*8*) and p-type GeTe alloys (*9*) are highly competitive to commercially available Bi_2Te_3 alloys (Figs. 3 and 4), making them possible alternatives for both thermoelectric cooling and power generation applications near room temperature.

RESULTS

Mathematical formulation of B_E

The electronic quality factor B_E can be defined for any pair of measurement of S and σ on the same sample at the same temperature according to Eq. 1 (detailed deduction is given in section S1)

$$B_E = S^2\sigma / \left[\frac{S_r^2 \exp(2 - S_r)}{1 + \exp[-5(S_r - 1)]} + \frac{S_r \pi^2/3}{1 + \exp[5(S_r - 1)]} \right],$$
$$\text{with } S_r = \frac{|S|}{k_B/e} \quad (1)$$

These measurements are routine for thermoelectric laboratories with the use of many commercial and custom-made systems (*10*). Equation 1 is motivated by relationship expected for a simple thermoelectric semiconductor. Equation 1 is well within 3% (typical experimental uncertainty) to the exact case of rigid, single parabolic band transport (including well converged multiple parabolic bands) with charges scattered by acoustic phonons (section S1). In real materials where these conditions are not exactly met, Eq. 1 can still be applied to give a value for B_E, only then it requires further interpretation, much like any other measured quantity. The numerators of the fractions in the sum correspond to the exact analytic solutions (*11*) of $S^2\sigma$ for a fully degenerate semiconductor (metal), $B_E S_r \pi^2/3$, and a fully nondegenerate semiconductor (lightly doped), $B_E S_r^2 \exp(2 - S_r)$. The denominators of the fractions are simply sigmoid functions to smoothly interpolate between these two analytic results. Note here that 5 and 1 in denominators of Eq. 1 are fitting parameters and the resultant fitting deviation is within 2.5%. The deviation can be minimized to be within 1.5% at fitting parameters of 5.33 and 1.09, rationalizing the use of 5 and 1 here for simplicity.

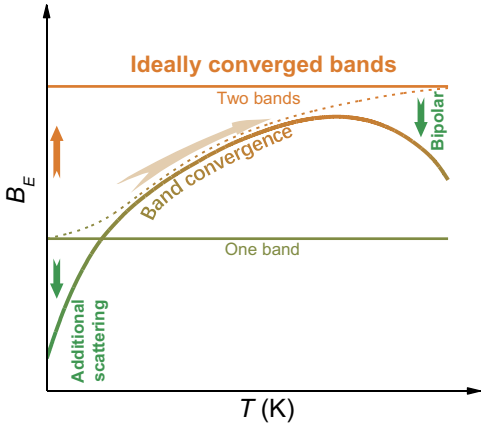

Fig. 2. Schematic temperature-dependent B_E. A model system involving a convergence of two identical bands, additional charge scattering, and a bipolar conduction.

Seebeck coefficient versus power factor

For each material, an average value for the electronic quality factor $\overline{B_E}$ can be treated as a scaling factor for $S^2\sigma$. More than 5000 data entries on scaled power factor, $S^2\sigma/\overline{B_E}$, for dozens of not necessarily optimized materials, both n-type and p-type, all fall on the same curve as a function of $|S|$ (Fig. 1), showing a mean deviation of only 3.6% (section S2). Since B_E has the dimension of the power factor, $S^2\sigma/\overline{B_E}$ is dimensionless. Note that $S^2\sigma$ has its maximum at a Seebeck coefficient of ~167 μV/K for each class of materials (section S2). This enables the conveniently accessible Seebeck coefficient to guide the electronic optimization, without knowing the carrier concentration (n), while, in tradition, $S^2\sigma$ optimization usually involves experimental variations in n in a broad range and the optimal n strongly depends on the band structure and temperature (*6*). Moreover, using Seebeck coefficient as a guidance is material and temperature independent.

The fact that all the data fit essentially on the same curve indicates that most of thermoelectric materials have qualitatively similar electronic transport, enabling their electronic properties to be characterized by a single-parameter B_E for each class of materials. B_E can be determined solely from a single simultaneous measurement of S and σ at any temperature from a degenerately doped sample that is not necessarily optimized. In short, this electronic scaling approach offers a clear revelation of the underlying universality in charge transport of thermoelectrics. Although "universality" strictly holds for SPB-APS materials, many known high-performance thermoelectric materials with a multiband conduction effectively

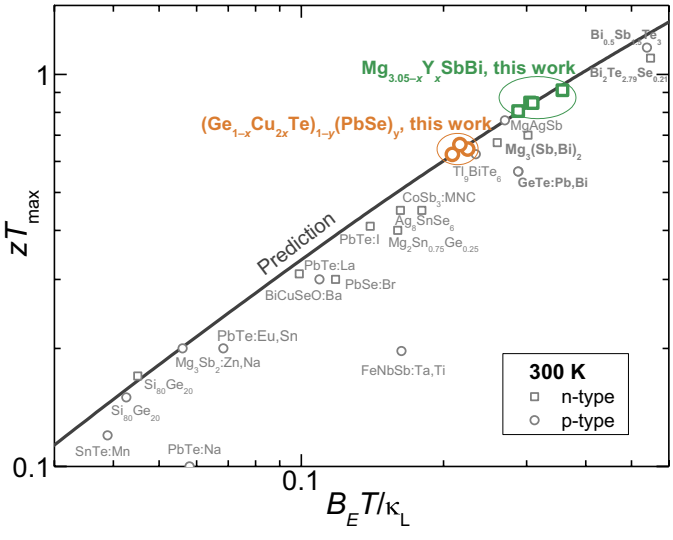

Fig. 3. Thermoelectric quality factor $B_E T/\kappa_L$ versus maximum zT (zT_{max}) at 300 K. $B_E T/\kappa_L$ is a good predictor for zT_{max} of an optimally doped sample. The solid curve shows the prediction, and the symbols stand for measurements. Detailed references are given in fig. S5.

follows the universality, due to the small-energy offsets between these conducting bands. Good examples are p-type PbTe at $T > 500$ K (fig. S4, 1jj), n-type filled skutterudites (fig. S4, 1T), and n-type $Mg_2(Si,Sn)$ (fig. S4, 2l). Note that B_E is anisotropic in anisotropic materials (fig. S4), although most of the data collected in this work are from polycrystalline materials that show isotropic electronic properties.

B_E as an indicator for thermoelectrics

B_E is not very temperature dependent because the material parameters that mostly affect B_E (section S3) such as effective mass and elastic constants all have weak temperature dependences. This may be unexpected, as the mobility of charge carriers drops quickly with increasing temperature due to the increase in phonon scattering. However, this decrease in σ is compensated by an increase in S. For an exact SPB-APS system, this compensation is exact and σ versus S at all temperatures and doping concentrations fall on the same curve for the same material class (section S2).

Because B_E is nearly a constant for good thermoelectric materials (SPB-APS), any deviation in B_E with temperature or doping can be used to indicate new effects such as band movement (*3*), additional charge scattering (*12*, *13*), and bipolar conduction (*14*), as schematically shown in Fig. 2 and section S3. Data showing observable deviations between predictions and measurements are shown in gray in fig. S5, with corresponding reasons marked. Note that among these effects, only band convergence enables an increase in B_E while the other two generally lead to a decrease.

Guiding the optimization of *zT*

B_E completely describes the electronic contribution to the thermoelectric quality factor via $B = B_E T/\kappa_L$ (sections S1 and S3) (*2*, *15*–*20*), and so, with the knowledge of lattice thermal conductivity (κ_L), it determines the maximum possible zT (zT_{max}) for a material (*2*). The mean deviation is only 3% between measured and predicted zT's using $B_E T/\kappa_L$ (section S3). Note that κ_L generally decreases with temperature (by T^{-1} to T^0; section S1), which explains why zTs are generally higher at high temperatures.

Most commercial thermoelectric devices operate near room temperature for cooling and low-grade waste-heat recovery, making the range of 200 to 500 K the most important. By comparing $B_E T/\kappa_L$ at 300 K (Fig. 3), it is seen that both p-type GeTe alloys and n-type Mg_3SbBi alloys are strong competitors to commercial

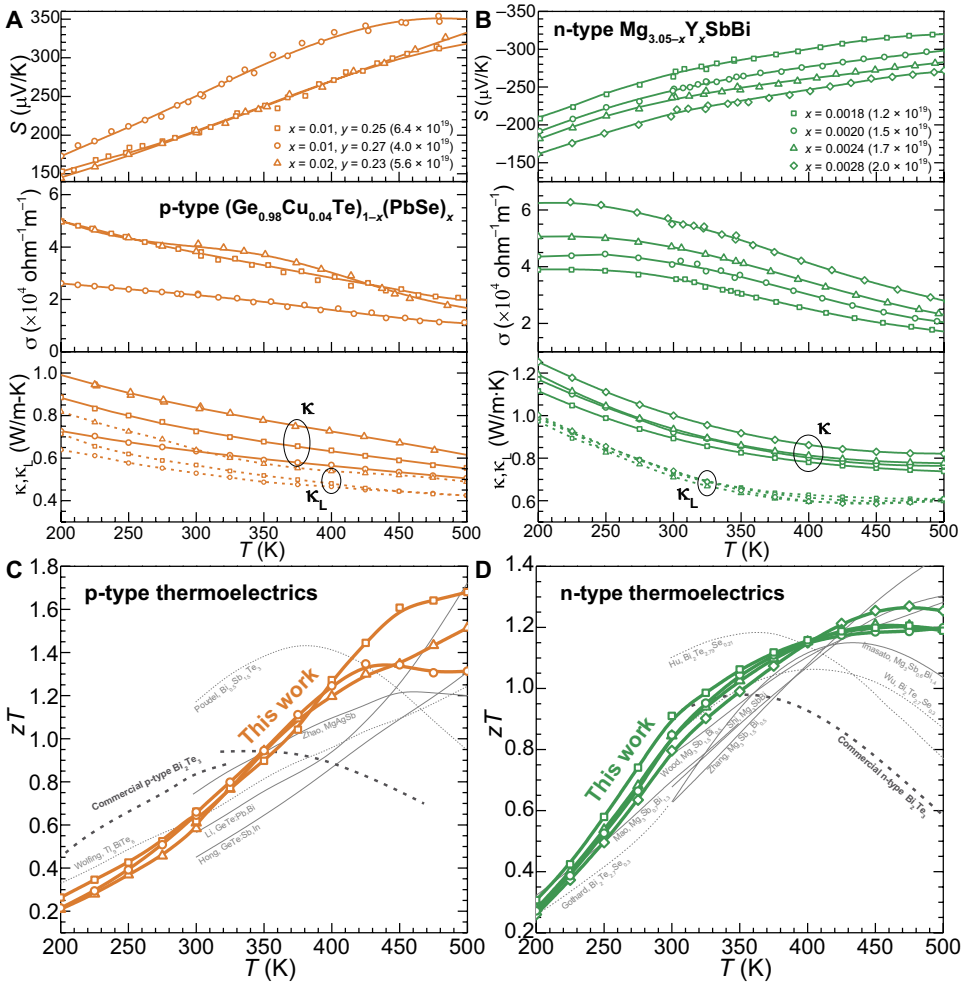

Fig. 4. Thermoelectric properties. Seebeck coefficient, electrical conductivity, thermal conductivity and its lattice component (**A** and **B**), and thermoelectric figure of merit zT (**C** and **D**) for p-type GeTe alloys and n-type Mg_3SbBi alloys, with a comparison to that of commercial Bi_2Te_3 and other high-performance thermoelectrics (*8*, *9*, *13*, *14*, *21*–*30*) in the temperature range of 200 to 500 K.

Bi_2Te_3-based alloys (note that Tl_9BiTe_6 and MgAgSb seem promising as well). However, existing studies have not fully optimized these materials for use in this important temperature range (*8*, *9*, *13*, *14*, *21*–*30*), and the lower than predicted experimentally realized peak zT indicates available improvements through a further optimization. Guided by the B_E developed in this work (section S3), a high thermoelectric performance in both n-type and p-type materials near room temperature is successfully realized (Fig. 4 and section S4), which is highly competitive to that of commercial Bi_2Te_3.

DISCUSSION

The electronic transport properties of good thermoelectrics can be understood by a simple relationship between the power factor and Seebeck coefficient through the thermoelectric electronic quality factor B_E. This material parameter is shown experimentally to be approximately a constant for all temperatures and doping within a class of thermoelectric semiconductors. Any deviation indicates new effects that help us understand and improve the materials. B_E entirely describes the electronic contribution to the thermoelectric quality factor $B = B_E T/\kappa_L$ and therefore characterizes the maximum thermoelectric figure of merit zT of a material.

Both B and B_E are based on the framework of SPB-APS, enabling the determination of the maximum zT and the maximum power factor, respectively. B_E offers a great advantage of its temperature independence, while, in general, B irregularly depends on temperature, enabling a useful tool for electronically guiding the screening and optimization of thermoelectrics with notably reduced experiment loads because B_E can be conveniently determined by any single pair of measurements of S and σ regardless of temperature and doping levels. Although the reality might deviate from the restrictions of SPB-APS (including complex, nonparabolic bands and various possible scattering assumptions), the capability of B_E on guiding the electronic optimization (thus, zT) is validated in most of known thermoelectric materials within interested broad temperature and composition ranges.

Guided by this approach, both p-type GeTe alloys and n-type Mg_3SbBi are revealed in this work as strong competitors to that of commercial Bi_2Te_3 for low-grade waste-heat recovery and refrigeration applications. This work not only offers an efficient strategy to maximize the zT of a given material but also enables a fast evaluation and screening of new thermoelectrics, with notably reduced loads on both synthesis and measurements.

MATERIALS AND METHODS

Synthesis

Polycrystalline $(Ge_{1-x}Cu_{2x}Te)_{1-y}(PbSe)_y$ ($x \leq 0.02$; $y = 0.23$, 0.25, and 0.27) samples were synthesized by melting the stoichiometric amount of high-purity elements (>99.99%) sealed in evacuated quartz ampoule at 1223 K for 10 hours and quenching in cold water, followed by annealing at 873 K for 48 hours with water quenching. For $Mg_{3.05-x}Y_xSbBi$ ($0.0018 \leq x \leq 0.0028$) samples, stoichiometric amounts of high-purity elements (>99.9%) of Mg, Y, Sb, and Bi were sealed in a tantalum container loaded in an evacuated quartz ampoule for melting at 1400 K for 6 hours, quenching in cold water, and then annealing at 873 K for 2 days. The tantalum tubes were sealed with an arc-melting system in argon with a pressure slightly lower than 1 atm. The obtained ingots of $(Ge_{1-x}Cu_{2x}Te)_{1-y}(PbSe)_y$ were then hand-ground into fine powders for hot pressing (*31*) at 850 K for 40 min under a uniaxial pressure of~80 MPa. To avoid oxidation during the grinding process, the ingots of $Mg_{3.05-x}Y_xSbBi$ were cut into big pieces (about 3 mm in size) for hot pressing (*31*) at 850 K for 40 min under a uniaxial pressure of ~110 MPa. The obtained pellets (>98% of the theoretical density) were ~12 mm in diameter and ~2 mm in thickness.

Transport property measurements

The Seebeck coefficient (S) was obtained from the slope of thermopower versus temperature gradient within 0 to 5 K. The resistivity (ρ) and Hall coefficient (R_H) were measured by a four-probe van der Pauw technique under a reversible superconductor magnetic field of 1.5 T. ρ, S, and R_H at 200 to 300 K were measured on pellets under helium with an Oxford cryostat (TeslatronTP). The thermal conductivity (κ) in the temperature range of 200 to 500 K is determined by $\kappa = dCpD$, where d is the density estimated by the measured mass/volume, Cp is heat capacity estimated by the Dulong-Petit approximation and it is assumed to be temperature independent, and D is the thermal diffusivity measured by a laser flash technique with a flowing liquid nitrogen coolant (NETZSCH LFA 467). The uncertainty in measurements of S, ρ, κ, and R_H is about 5%.

SUPPLEMENTARY MATERIALS

Supplementary material for this article is available at http://advances.sciencemag.org/cgi/content/full/6/46/eabc0726/DC1

REFERENCES AND NOTES

1. L. E. Bell, Cooling, heating, generating power, and recovering waste heat with thermoelectric systems. *Science* **321**, 1457–1461 (2008).
2. H. J. Goldsmid, *Introduction to Thermoelectricity* (Springer, 2009).
3. Y. Pei, X. Shi, A. LaLonde, H. Wang, L. Chen, G. J. Snyder, Convergence of electronic bands for high performance bulk thermoelectrics. *Nature* **473**, 66–69 (2011).
4. Y. Pei, A. D. LaLonde, H. Wang, G. J. Snyder, Low effective mass leading to high thermoelectric performance. *Energ. Environ. Sci.* **5**, 7963–7969 (2012).
5. Y. I. Ravich, B. A. Efimova, I. A. Smirnov, *Semiconducting Lead Chalcogenides* (Monographs in Semiconductor Physics v.5, Plenum Press, 1970), p. xv.
6. Y. Pei, Z. M. Gibbs, B. Balke, W. G. Zeier, G. J. Snyder, Optimum carrier concentration in n-type PbTe thermoelectrics. *Adv. Energy Mater.* **4**, 1400486 (2014).
7. G. J. Snyder, E. S. Toberer, Complex thermoelectric materials. *Nat. Mater.* **7**, 105–114 (2008).
8. X. Shi, T. Zhao, X. Zhang, C. Sun, Z. Chen, S. Lin, W. Li, H. Gu, Y. Pei, Extraordinary n-type Mg_3SbBi thermoelectrics enabled by yttrium doping. *Adv. Mater.* **31**, 1903387 (2019).
9. J. Li, X. Zhang, Z. Chen, S. Lin, W. Li, J. Shen, I. T. Witting, A. Faghaninia, Y. Chen, A. Jain, L. Chen, G. J. Snyder, Y. Pei, Low-symmetry rhombohedral gete thermoelectrics. *Joule* **2**, 976–987 (2018).
10. K. A. Borup, J. de Boor, H. Wang, F. Drymiotis, F. Gascoin, X. Shi, L. D. Chen, M. I. Fedorov, E. Muller, B. B. Iversena, G. J. Snyder, Measuring thermoelectric transport properties of materials. *Energ. Environ. Sci.* **8**, 423–435 (2015).
11. A. Zevalkink, D. M. Smiadak, J. L. Blackburn, A. J. Ferguson, M. L. Chabinyc, O. Delaire, J. Wang, K. Kovnir, J. Martin, L. T. Schelhas, T. D. Sparks, S. D. Kang, M. T. Dylla, G. J. Snyder, B. R. Ortiz, E. S. Toberer, A practical field guide to thermoelectrics: Fundamentals, synthesis, and characterization. *Appl. Phys. Rev.* **5**, 021303 (2018).
12. J. Zhou, H. Zhu, T. H. Liu, Q. Song, R. He, J. Mao, Z. Liu, W. Ren, B. Liao, D. J. Singh, Z. Ren, G. Chen, Large thermoelectric power factor from crystal symmetry-protected non-bonding orbital in half-Heuslers. *Nat. Commun.* **9**, 1721 (2018).
13. M. Wood, J. J. Kuo, K. Imasato, G. J. Snyder, Improvement of low-temperature zT in a Mg_3Sb_2-Mg_3Bi_2 solid solution via Mg-vapor annealing. *Adv. Mater.* **31**, 1902337 (2019).
14. D. Chung, T. Hogan, P. Brazis, M. Rocci-Lane, C. Kannewurf, M. Bastea, C. Uher, M. G. Kanatzidis, $CsBi_4Te_6$: A high-performance thermoelectric material for low-temperature applications. *Science* **287**, 1024–1027 (2000).
15. Y. Pei, H. Wang, G. J. Snyder, Band engineering of thermoelectric materials. *Adv. Mater.* **24**, 6125–6135 (2012).

16. G. D. Mahan, in *Solid State Physics*, H. Ehrenreich, F. Spaepen, Eds. (Academic Press Inc., 1998), vol. 51, pp. 81–157.
17. G. A. Slack, in *CRC Handbook of Thermoelectrics*, D. M. Rowe, Ed. (CRC Press, 1995), chap. 34, pp. 406–440.
18. J. Yan, P. Gorai, B. Ortiz, S. Miller, S. A. Barnett, T. Mason, V. Stevanović, E. S. Toberer, Material descriptors for predicting thermoelectric performance. *Energ. Environ. Sci.* **8**, 983–994 (2015).
19. H. Wang, Y. Pei, A. D. LaLonde, G. Jeffery Snyder, in *Thermoelectric Nanomaterials: Materials Design and Applications*, K. Koumoto, T. Mori, Eds. (Springer, 2013), pp. 3–32.
20. Y. Xiao, D. Wang, Y. Zhang, C. Chen, S. Zhang, K. Wang, G. Wang, S. J. Pennycook, G. J. Snyder, H. Wu, L. D. Zhao, Band sharpening and band alignment enable high quality factor to enhance thermoelectric performance inn-type PbS. *J. Am. Chem. Soc.* **142**, 4051–4060 (2020).
21. D. Kraemer, J. Sui, K. McEnaney, H. Zhao, Q. Jie, Z. F. Ren, G. Chen, High thermoelectric conversion efficiency of MgAgSb-based material with hot-pressed contacts. *Energ. Environ. Sci.* **8**, 1299–1308 (2015).
22. M. Hong, Z. G. Chen, L. Yang, Y. C. Zou, M. S. Dargusch, H. Wang, J. Zou, Realizing zT of 2.3 in $Ge_{1-x-y}Sb_xIn_yTe$ via reducing the phase-transition temperature and introducing resonant energy doping. *Adv. Mater.* **30**, 1705942 (2018).
23. B. Wolfing, C. Kloc, J. Teubner, E. Bucher, High performance thermoelectric Tl_9BiTe_6 with an extremely low thermal conductivity. *Phys. Rev. Lett.* **86**, 4350–4353 (2001).
24. B. Poudel, Q. Hao, Y. Ma, Y. C. Lan, A. Minnich, B. Yu, X. A. Yan, D. Z. Wang, A. Muto, D. Vashaee, X. Y. Chen, J. M. Liu, M. S. Dresselhaus, G. Chen, Z. F. Ren, High-thermoelectric performance of nanostructured bismuth antimony telluride bulk alloys. *Science* **320**, 634–638 (2008).
25. H. Zhao, J. Sui, Z. Tang, Y. Lan, Q. Jie, D. Kraemer, K. McEnaney, A. Guloy, G. Chen, Z. Ren, High thermoelectric performance of MgAgSb-based materials. *Nano Energy* **7**, 97–103 (2014).
26. K. Imasato, S. D. Kang, G. J. Snyder, Exceptional thermoelectric performance in $Mg_3Sb_{0.6}Bi_{1.4}$ for low-grade waste heat recovery. *Energy Environ. Sci.* **12**, 965–971 (2019).
27. J. Mao, H. Zhu, Z. Ding, Z. Liu, G. A. Gamage, G. Chen, Z. Ren, High thermoelectric cooling performance of n-type Mg_3Bi_2-based materials. *Science* **365**, 495–498 (2019).
28. L. Hu, H. Wu, T. Zhu, C. Fu, J. He, P. Ying, X. Zhao, Tuning multiscale microstructures to enhance thermoelectric performance of n-type bismuth-telluride-based solid solutions. *Adv. Energy Mater.* **5**, 1500411 (2015).
29. N. Gothard, X. Ji, J. He, T. M. Tritta, Thermoelectric and transport properties of n-type Bi_2Te_3 nanocomposites. *J. Appl. Phys.* **103**, 054314 (2008).
30. Y. Wu, Y. Yu, Q. Zhang, T. Zhu, R. Zhai, X. Zhao, Liquid-phase hot deformation to enhance thermoelectric performance of n-type bismuth-telluride-based solid solutions. *Adv. Sci.* **6**, 1901702 (2019).
31. A. D. LaLonde, T. Ikeda, G. J. Snyder, Rapid consolidation of powdered materials by induction hot pressing. *Rev. Sci. Instrum.* **82**, 025104 (2011).

Acknowledgments

Funding: This work is supported by the National Natural Science Foundation of China (grant no. 51772215, 51861145305) and the National Key Research and Development Program of China (2018YFB0703600). G.J.S. and M.W. acknowledge the support of US-DOE, award no. 197455//DE-AC02-76SF00515. **Author contributions:** Y.P. conceptualized this work. X.Z., Z.B., and X.S. carried out the experiments. X.Z., Z.C., S.L., and B.S. collected literature data. M.W., A.H.S., and G.J.S deduced the mathematical formulation of B_E. X.Z., L.C., G.J.S., and Y.P. wrote the manuscript. All authors discussed the results and provided feedback on the manuscript. **Competing interests:** The authors declare that they have no competing interests. **Data and materials availability:** All data needed to evaluate the conclusions in the paper are present in the paper and/or the Supplementary Materials. Additional data related to this paper may be requested from the authors.

Submitted 4 April 2020
Accepted 1 October 2020
Published 13 November 2020
10.1126/sciadv.abc0726

Citation: X. Zhang, Z. Bu, X. Shi, Z. Chen, S. Lin, B. Shan, M. Wood, A. H. Snyder, L. Chen, G. J. Snyder, Y. Pei, Electronic quality factor for thermoelectrics. *Sci. Adv.* **6**, eabc0726 (2020).

Science Advances

Electronic quality factor for thermoelectrics

Xinyue Zhang, Zhonglin Bu, Xuemin Shi, Zhiwei Chen, Siqi Lin, Bing Shan, Maxwell Wood, Alemayouh H. Snyder, Lidong Chen, G. Jeffrey Snyder and Yanzhong Pei

Sci Adv **6** (46), eabc0726.
DOI: 10.1126/sciadv.abc0726